Microwave assisted synthesis and characterisation of divalent metal tungstate nanocrystalline minerals: ferberite, hübnerite, sanmartinite, scheelite and stolzite

J. Theo Kloprogge*, Matt L. Weier, Loc V. Duong, and Ray L. Frost

Inorganic Materials Research group. School of Physical and Chemical Sciences. Queensland University of Technology, GPO Box 2434, Brisbane, Q 4001, Australia

Published as:
Kloprogge, J.T., Weier, M.L., Martens, W.N. and Frost, R.L. (2004) Microwave assisted synthesis of divalent metal tungstate minerals: ferberite, hübnerite, sanmartinite, scheelite and stolzite. Materials Chemistry and Physics, 88(2-3), 438-443.

Abstract

A variety of metal tungstates have been synthesised in a microwave assisted oven at 100 and 150˚C and corresponding autogenous water vapour pressure within a time frame of 30 minutes to 2 hours. The crystals formed are of submicrometer size and show equidimensional and needle-like crystals. Increasing the synthesis time and temperature results in the disappearance of the needles and the growth of the equidimensional crystals. The Raman spectra are consistent with those reported for the natural equivalents of these tungstates. The lead tungstate $\nu_1(A_g)$ mode is observed at 904 cm^{-1}, while the $\nu_2(A_g)$ vibration is observed as a strong band at at 326 cm^{-1} accompanied by a weak $\nu_2(B_g)$. at 356 cm^{-1}. The $\nu_3(B_g)$ vibration is located around 741 cm^{-1}, whereas the $\nu_3(E_g)$ is found at 751 cm^{-1}. Finally, the $\nu_4(B_g)$ vibration is completely overlapping with the $\nu_2(A_g)$ vibration. The band around 271 cm^{-1} may be the equivalent of the infrared active $\nu_4(A_u)$ activated due to strain in the crystal. The two bands at 190 and 177 cm^{-1} are ascribed to the ν(Pb-O) and as a translational mode of the WO_4 group in stolzite.

Introduction

The major natural tungsten ores are formed by the minerals scheelite, $CaWO_4$, and wolframite $(Fe,Mn)WO_4$ with its endmembers ferberite and hübnerite. Depending on the size of the cation tungstates can crystallize in either the scheelite or the wolframite structure. Scheelite structures with the tungsten in tetrahedral coordination are formed with large bivalent cations like Ca, Ba, Pb and Sr. Alternatively, with smaller bivalent cations (Fe, Mn, Co, Ni, Mg, Zn) the wolframite structure will be formed with the tungsten in octahedral coordination.

Lead tungstate is found in nature as two dimorphous minerals as the result of hydrothermal formation, metasomatism and oxidation of primary lead ore minerals [1-9]. The tetragonal form stolzite and the monoclinic form raspite. Stolzite, named after J. Stolz from the Czech Republic, forms dipyramidal crystals, often thick tabular with striated faces. Stolzite has a crystal structure similar to that of scheelite with the Pb^{2+} in 8-coordination with $(WO_4)^{2-}$ groups. The tungstate tetrahedra are slightly flattened along the *c*-axis and join edges with PbO_8. In this group Ca and Pb may substitute for each other resulting in a partial series between scheelite, $CaWO_4$, and

stolzite, $PbWO_4$. The substitution of W by Mo results in another partial series between stolzite and wulfenite, $PbMoO_4$ [10].

Lead tungstate has been attracting some interest recently because it forms an important inorganic scintillating crystal since it was approved for application in the the Compact Muon Solenoid (CMS) and Assembly Line Balance (ALICE) experiments to construct a precision electron-magnetic calorimeter at the Large Hydron Collider (LHC) [11-16]. Because stolzite has the tetragonal scheelite structure it can be expected that it will be a good oxide ion conductor. It has been shown that doping lead tungstate with rare earth elements results in ion conductivity. Ihn et al. [17] reported on the use of three component Ag_2S-PbS-$PbWO_4$ electrodes for potentiometric analysis of tungsten. Kaminskii et al. [18] described the use of $PbWO_4$ as oscillators for nanosecond Raman lasing, which might be usefull for applications such as the generation of wavelength in the UV range (in conjunction with other nonlinear processes) for ozone differential absorption lidar. This material has optical transparency from approximately 0.33 to approximately 5.5 μm, making it also potentially useful for trace gas detection in the IR.

Raman spectroscopy is often used for the study of tungstates and molybdates. Daturi et al. (1997) described the synthesis of mixed oxide powders in the system $CdMo_xW_{1-x}O_4$. They found that for $x < 0.25$ virtually pure wolframite-type structures were formed, whereas at $x > 0.75$ virtually pure scheelite-type structures were formed. Furthermore Raman spectroscopy is regularly used to study the effects of incorporating a diversity of metals for example of interest for catalysis [19-22] and alkaline and rare earth elements [19].

In associated work we have described the synthesis and characterisation of the related lead sulphate anglesite and chromate crocoite [23]. We also reported on the naturally occurring lead molybdate chillagite [24] and on the Raman spectroscopy of scheelite, wolframite and wulfenite [25]. This work is a continuation of our research in this group of minerals and their applications. So far a variety of methods have been used to synthesise tungstates including hydrothermal synthesis, high temperature solid-state synthesis, flux methods, reaction of oxides with WO_3 vapor, mechanochemical activation and cooling from melts [26-37]. However, to our knowledge microwave assisted synthesis has not been described so far for lead tungstate.In this paper we describe in details the microwave assisted synthesis and characterization of selected divalent metal tungstates that crystallize either with the scheelite or with the wolframite structure.

Experimental

Microwave assisted hydrothermal synthesis

The metal tungstates were hydrothermally synthesised by mixing analytical grade sodium tungstate and the required metal (Fe, Mn, Zn, Pb, Ca) nitrate. In each synthesis 0.05 M of both compounds were mixed in 100 ml deionized water. A little excess of tungstate was added [26]. These solutions were added into Teflon-lined beakers with lid inside a high density polypropylene rotor (Fig. 1) for treatment in a MicroSYNTH Microwave Labstation controlled by a Labterminal 800 Controller (Milestone Microwave Laboratory Systems). The samples were heated from room temperature to 150°C in 4 minutes, kept at 150° under autogeneous water vapour pressure for 1 hour followed by cooling under a cold airflow. An optical fiber temperature sensor controls the power generated by the Microwave Labstation in order to maintain the required temperature profile. A pressure sensor measures the

pressure inside the vessel and acts as a safety in case that the pressure increases above a set threshold. During the synthesis the vessels rotate inside the Microwave Labstation in order to get homogeneous heating. Inside each vessel a magnetic stirrer provides adequate mixing of the compounds. Additional Pb-tungstate sample solutions were heated from room temperature to 100° and 150°C in 4 minutes, kept at 100° or 150° for 0.5, 1 and 2 hours followed by cooling under a cold air flow. The precipitates were collected, filtered and washed with deionized water.

Analytical techniques

After drying phase identification was conducted by X-ray Diffraction (XRD) using a Philips wide-angle PW 1050/25 vertical goniometer applying CuKα radiation. The samples were measured in stepscan mode with steps of 0.02° 2θ and a scan speed of 1.00° per minute from 5 to 75°2θ.

To obtain the Raman spectra the samples were placed on a polished metal surface on the stage of an Olympus BHSM microscope, which is equipped with 10x, 20x, and 50x objectives. The microscope is part of a Renishaw 1000 Raman microscope system, which also includes a monochromator, a filter system and a CCD detector (1024 pixels). The Raman spectra were excited by a Spectra-Physics model 127 He-Ne laser producing highly polarized light at 633 nm and collected at a resolution of 2 cm^{-1} and a precision of ± 1 cm^{-1} in the range between 200 and 4000 cm^{-1}. Repeated acquisition on the crystals using the highest magnification (50x) were accumulated to improve the signal to noise ratio in the spectra. Spectra were calibrated using the 520.5 cm^{-1} line of a silicon wafer. Baseline adjustment, smoothing and normalization were performed using the Spectracalc software package GRAMS (Galactic Industries Corporation, NH, U.S.A.). Band component analysis was carried out using the peakfit software package by Jandel Scientific. Lorentz-Gauss cross product functions were used throughout and peakfitting was carried out until squared correlation coefficients with $r^2 > 0.995$ were obtained.

Scanning electron microscope (SEM) images were obtained on a FEI QUANTA 200 Environmental Scanning Electron Microscope operating in this case at high vacuum and 20 kV.

Results and discussion

The XRD patterns of the scheelite and stolzite are much sharper and stronger in intensity than those of the other tungstates (Fig.2a). Clearly the minerals with the scheelite structure are more crystalline. This is probably related to the conditions under which these minerals form in nature. Scheelite generally occurs in contact metamorphic deposits known as skarns, where granitic intrusions have become in contact with limestones. In contrast, wolframite is found associated with quartz in veins in the peripheral areas of granitic bodies, deposited by hydrothermal solutions.

Fig. 2b shows the XRD patterns of the lead tungstate samples synthesised under varying conditions. All peaks visible in the diffraction pattern are consistent with the tetragonal form of lead tungstate, stolzite. The unit cell parameters determined from the diffraction pattern are, within the experimental error, in close agreement with those reported for natural stolzite and synthetic lead tungstate. The reflections are very sharp and following the Scherrer equation this indicates that the crystallites are in general between 0.1 and 1 micron in size. With increasing time and temperature the reflections in the XRD patterns are getting sharper indicating the growth of the crystallites due to Ostwald ripening.

The lead-tungstate sample synthesised at 100˚C for 1 hour shows small equidimensional crystals of stolzite together with dendrite-like aggregates formed by growth small crystals perpendicular to a common axis in four more or less perpendicular directions (Fig 3). The crystals, although very small and of submicrometer size, exhibit a morphology dominated by prisms and a terminating pyramid. This is consistent with the fact that stolzite under natural conditions tends to form tabular dipyramidal crystals. Under the microwave synthesis conditions the crystals all have their c-axis perpendicular to the log's axis and individual crystals are not joint parallel to the prismatic faces. Increasing the synthesis temperature results in the disappearance of most of the dendrites and the formation of much larger more or less equidimensional crystallites. The few whiskers that did surface have grown in size and the crystals all have now a sintered look making the observation of the prism faces impossible. Application of a shorter synthesis time of 30 minutes at 100˚C (Fig. 3a) results in the formation of a mixture of small needles and equidimensional crystals of only a few tenth of a micron in size. In this sample dendrites were also observed. Increasing the synthesis time to 1 and 2 hrs (Fig. 3b and c) and increasing the synthesis temperature to 150°C strongly diminishes the number of dendrites present, but the ones that are still present grow and at 150°C the crystals actually seem to sinter together (Fig. 3d).

It is thought that the original needles formed in the first 30 minutes act as the seed for the formation of the logs with the new crystals growing epitaxially on its surface. Unfortunately due to its very small size and the complete overgrowth with the new crystals the presence of a central needle could not be confirmed. In conclusion it can be said that this is the first time that the formation of lead tungstate dendrites has been described.

Fig. 4 shows the Raman spectrum of the synthetic tungstates. Minerals with a scheelite structure like scheelite itself and stolzite have site group S_4 and space group C^6_{4h}. The crystal structure resembles that of zircon and therefore the WO_4 groups should show four bands only in the Raman spectra, two components each of ν_3 and ν_4. The scheelite structure has been shown to be one of the few for which the correlation splitting of the internal modes has been observed. This results in ν_1: A_g(R) + B_u(inactive), ν_2: A_g + B_g(R) +A_u(ir) +B_u, ν_3, ν_4: B_g + E_g(R) + A_u(ir) + E_u(ir) [39]. Raman spectroscopy is quite often used for the study of synthetic tungstates and molybdates. Daturi et al. [40] have described the preparation of mixed oxide powders in the system $CdMo_xW_{1-x}O_4$. They found that for $x \leq 0.25$ virtually pure wolframite-type structures were formed whereas at $x \geq 0.75$ virtually pure scheelite-type structures were formed. Furthermore Raman spectroscopy is regularly used to study the effects of incorporating a large diversity of metals for example of interest for catalysis [19-22, 41] and alkaline and rare earth elements [19]. In situ X-ray diffraction and Raman spectroscopy in diamond anvil cells has been applied to study phase transitions in scheelite-type materials as a function of pressure [41].

For scheelite the $\nu_1(A_g)$ band is observed at 909 cm^{-1} and although the corresponding $\nu_1(B_u)$ vibration should be inactive a minor band is observed around 894 cm^{-1} due to strain in the crystal [39]. The corresponding $\nu_1(A_g)$ mode for stolzite is observed at 904 cm^{-1}. The $\nu_2(A_g)$ vibration is observed as a strong band at 330 cm^{-1} for scheelite and at 326 cm^{-1} for stolzite accompanied by a weak $\nu_2(B_g)$ at 400 cm^{-1} and 356 cm^{-1} for scheelite and stolzite respectively. The scheelite $\nu_3(B_g)$ vibration is located around 836 cm^{-1}, whereas the $\nu_3(E_g)$ is found at 795 cm^{-1}. Similar bands are observed for the stolzite at 764 and 751 cm^{-1}. The $\nu_4(B_g)$ vibration is completely

overlapping with the $\nu_2(A_g)$ vibration. The $\nu_4(E_g)$ is absent in the scheelite spectrum. The band at 271 cm^{-1} may be the equivalent of the infrared active $\nu_4(A_u)$ activated due to strain in the crystal. However, Daturi et al. [40] assigned a similar band at 273 cm^{-1} as a Raman active $\nu(B_g)$ mode for scheelite-type $CdMoO_4$. This band is not observed for stolzite. The bands at 193 and 208 cm^{-1} can be assigned to translational modes ν(Ca-O) and the 193 cm^{-1} band maybe also as a translational mode of the WO_4 group in scheelite [21, 40]. In a similar way the bands at 190 and 177 cm^{-1} can be ascribed to the ν(Pb-O) and as a translational mode of the WO_4 group in stolzite.

Hübnerite reveals a medium strong band at 127 cm^{-1} accompanied by weak bands at 162 and 173 cm^{-1}, which are ascribed to interchain deformation and torsion modes [42]. The band at 201 cm^{-1} has been described for $ZnWO_4$ at 199 cm^{-1} as $\nu(A_g)$ involving the Zn cation [19]. The band at 255 cm^{-1} identical to 273 cm^{-1} band for sanmartinite is assigned as the $\nu_{def}(A_g)$ of the cationic sublattices. Fomichev & Kondratov [19] ascribed the bands at 353 and 395 cm^{-1} as deformation modes, whereas Daturi et al. [40] assigned them as $r(B_g)$ and $\delta(A_g)$ modes of terminal WO_2 groups. The band at 510 cm^{-1} is assigned as the $\nu_{sym}(B_g)$ mode of the $(W_2O_4)_n$ chain with the symmetric A_g mode at 543 cm^{-1}. The bands at 678 and 697 cm^{-1} are equivalent to the $\nu_{as}(A_g)$ and $\nu_{as}(B_g)$ mode of the $(W_2O_4)_n$ chain observed at 687 and 706 cm^{-1} respectively for $CdWO_4$ [40] and at 675 and 705 cm^{-1} for sanmartinite. The bands at 774 and 886 cm^{-1} are associated with the antisymmetric and symmetric B_g and A_g modes respectively of the terminal WO_2 groups [40]. The Raman spectrum of sanmartinite is in general very similar to that of hübnerite, except for the strong A_g mode at 886 cm^{-1}, which has shifted to 904 cm^{-1}. The spectrum of ferberite could not be obtained due to fluorescence.

In summary, all divalent metal tungstates with either the scheelite or the wolframite structure are easily synthesized using a microwave oven, especially in comparison with conventional techniques. The crystallinity of the scheelite group minerals is higher than that of the wolframite group minerals under the same synthesis conditions. In addition, this work shows that changes in morphology are not only caused by the presence of various anions as reported by An et al. [26], but also by the changes in time and temperature associated with the changes in autogenous water vapour pressure.

Acknowledgements

The financial support and infrastructure of the Queensland University of Technology, School of Physical and Chemical Sciences is gratefully acknowledged.

References

1. **M. N. AL'BOV, *Zapiski Vsesoyuz. Mineralog. Obshckestva (Mem. soc. russe mineral.)* 83 (1954) 148.**
2. **M. N. CHUREVA, *Zapiski Vsesoyuz. Mineral. Obshchestva (Mem. soc. russe mineral.)* 77 (1948) 103.**
3. **E. E. FOORD and N. M. CONKLIN, *Mineral. Rec.* 13 (1982) 149.**
4. **T. I. GETMANSKAYA, E. G. RYABEVA and K. V. YURKINA, *Nov. Dannye Miner.* 30 (1982) 183.**

5. S. P. KILIAS and J. KONNERUP-MADSEN, *Mineralium Deposita* 32 (1997) 581.
6. A. KOSAKEVITCH, *Morocco Miner. Ind. Mines, Direct. Mines Geol, Notes Mem. Serv. Geol.* No. 225 (1970) 179.
7. J. S. STEVENSON, *Univ. Toronto Studies, Geol. Ser.* No. 46 (1941) 137.
8. K. WALENTA, *Aufschluss* 26 (1975) 369.
9. L. K. YAKHONTOVA, *Zapiski Vsesoyuz. Mineralog. Obshchestva (Mem. soc. russe mineral.)* 83 (1954) 117.
10. C. KLEIN, *The 22nd edition fo the manual of mineral science (after James D. Dana)*, John Wiley & Sons, Inc., New York, 2002.
11. *CERN/LHCC 94-38* (1994).
12. M. NIKL, K. NITSCH, J. HYBLER, J. CHVAL and P. REICHE, *Phys. Status Solidi* 196 (1996) K7.
13. A. N. ANNEKOV, M. KORZHIK and P. LECOQ, *IEEE Nuclear Science Symposium Conference Record, Toronto, Nov. 8-14, 1998* 1 (1999) 46.
14. N. A. BAJANOV, Y. S. BLINNIKOV, Y. I. GUSEV, T. Y. KLECHNEVA, A. I. KOVALEV, L. A. LEVTCHENKO, F. V. MOROZ, D. M. SELIVERSTOV, V. A. KACHANOV, N. A. GOLUBEV, V. A. FROLOV, V. N. LUKYANOV, G. A. MAMAEVA and D. M. PRILUTSKAYA, *Nuclear Instruments & Methods in Physics Research, Section A: Accelerators, Spectrometers, Detectors, and Associated Equipment* 442 (2000) 146.
15. M. DIEMOZ, *Calorimetry in High Energy Physics, Proceedings of the International Conference, 8th, Lisbon, Portugal, June 13-19, 1999* (2000) 250.
16. M. KORZHIK and P. LECOQ, *IEEE Transactions on Nuclear Science* 48 (2001) 628.
17. G. S. IHN, J. H. LEE and R. P. BUCK, *Taehan Hwahakhoe Chi* 27 (1983) 111.
18. A. A. KAMINSKII, C. L. MCCRAY, H. R. LEE, S. W. LEE, D. A. TEMPLE, T. H. CHYBA, W. D. MARSH, J. C. BARNES, A. N. ANNANENKOV, V. D. LEGUN, H. J. EICHLER, G. M. A. GAD and K. UEDA, *Optics Communications* 183 (2000) 277.
19. V. V. FOMICHEV and O. I. KONDRATOV, *Spectrochim. Acta, Part A* 50A (1994) 1113.
20. J. HANUZA, K. HERMANOWICZ, W. RYBA-ROMANOWSKI, H. DRULIS and E. I. USPENSKY, *Pol. J. Chem.* 68 (1994) 185.
21. J. HANUZA, A. BENZAR, A. HAZNAR, M. MACZKA, A. PIETRASZKO and J. H. VAN DER MAAS, *Vib. Spectrosc.* 12 (1996) 25.
22. J. HANUZA, A. HAZNAR, M. MACZKA, A. PIETRASZKO, A. LEMIEC, J. H. VAN DER MAAS and E. T. G. LUTZ, *J. Raman Spectrosc.* 28 (1997) 953.
23. M. J. CRANE, P. LEVERETT, L. R. SHADDICK, P. A. WILLIAMS, J. T. KLOPROGGE and R. L. FROST, *N. Jb. Mineral., Mh.* (2001) 505.
24. M. J. CRANE, R. L. FROST, P. A. WILLIAMS and J. T. KLOPROGGE, *J. Raman Spectros.* 33 (2002) 62.
25. J. T. KLOPROGGE and R. L. FROST, *N. Jb. Mineral., Mh.* (1999) 193.
26. C. AN, K. TANG, G. SHEN, C. WANG and Y. QIAN, *Materials Letters* 57 (2002) 565.

27. **A. N. ANENKOV, M. V. KORZHIK, V. L. KOSTYLEV and V. D. LIGUN, in *Russ.*, (Russia). Ru, 2001, p. No pp. given.**
28. **I. N. BELYAEV, V. S. FILIP'EV and E. G. FESENKO, *Zh. Strukt. Khim.* 4 (1963) 719.**
29. **S. BURACHAS, V. MARTYNOV, V. RYZHIKOV, G. TAMULAITIS, H. H. GUTBROD and V. I. MANKO, *Journal of Crystal Growth* 186 (1998) 175.**
30. **G. CESARO, *Ann. soc. geol. Belg.* 37 (1911) 81.**
31. **J. HAN, G. ZHOU, F. LIU, S. ZHANG, Z. CHENG, J. HE and H. CHEN, *Progress in Crystal Growth and Characterization of Materials* 40 (2000) 167.**
32. **A. S. KHIM, J. WANG and X. JUNMIN, *Solid State Ionics* 132 (2000) 55.**
33. **T. NAKAMURA, K. SUGIYAMA, E. MORIGUCHI and T. SHOJI, *Shigen to Sozai* 118 (2002) 217.**
34. **N. SAITO, A. KUDO and T. SAKATA, *Bulletin of the Chemical Society of Japan* 69 (1996) 1241.**
35. **S.-H. WANG, D.-Z. SHEN, G.-H. REN, H.-H. NI, H. WU and Z.-W. YIN, *Wuji Cailiao Xuebao* 14 (1999) 847.**
36. **R. YUAN, E. SHI, W. LI, Y. ZHENG, N. WU and W. ZHONG, *Science in China, Series E: Technological Sciences* 43 (2000) 495.**
37. **V. V. ZYRYANOV, *Inorganic Materials (Translation of Neorganicheskie Materialy)* 36 (2000) 54.**
38. **J. T. KLOPROGGE and R. L. FROST, *N. Jb. Miner. Mh.* Mai (1999).**
39. **S. D. ROSS, *Inorganic Infrared and Raman Spectra*, McGraw-Hill Book Company, London, 1972.**
40. **M. DATURI, G. BUSCA, M. M. BOREL, A. LECLAIRE and P. PIAGGIO, *J. Phys. Chem. B* 101 (1997) 4358.**
41. **A. JAYARAMAN, S. K. SHARMA and S. Y. WANG, *J. Raman Spectrosc.* 29 (1998) 305.**
42. **J. P. LESNE and P. CAILLET, *Ann. Chim. (Paris)* 9 (1974) 57.**

.

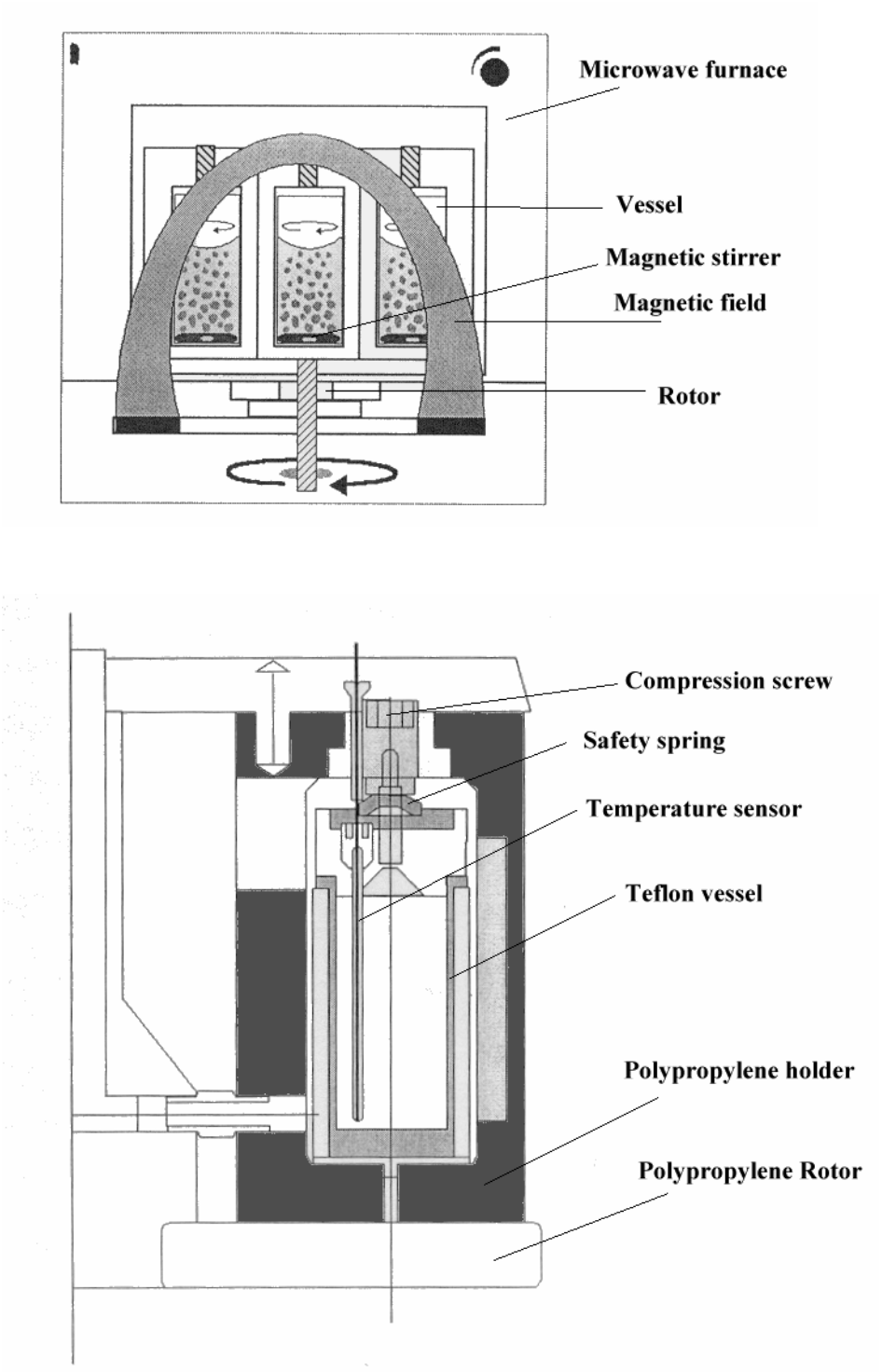

Fig. 1

Fig.1 Overview of the Microwave furnace and vessels.

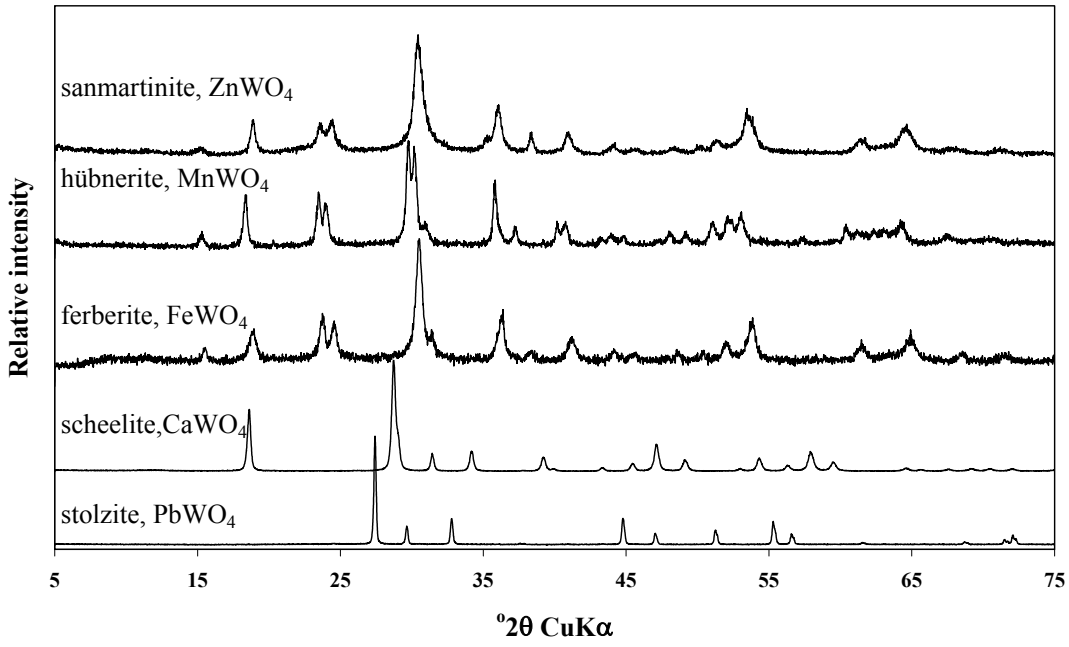

Fig. 2a XRD patterns of the synthetic tungstates

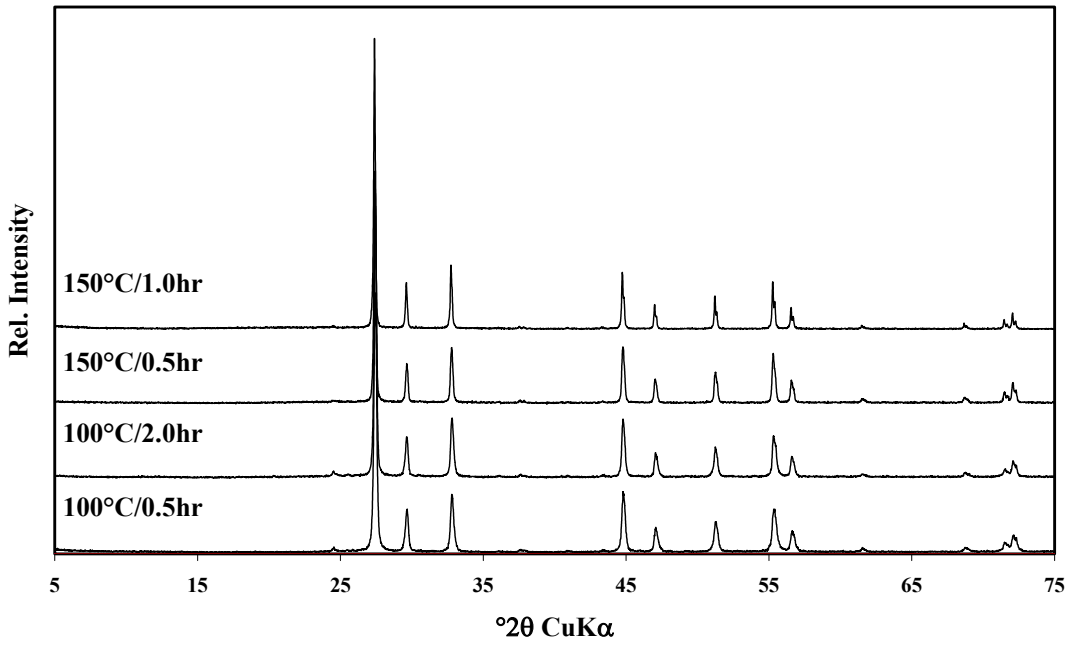

Fig. 2b XRD patterns of the microwave assisted synthesised lead tungstate.

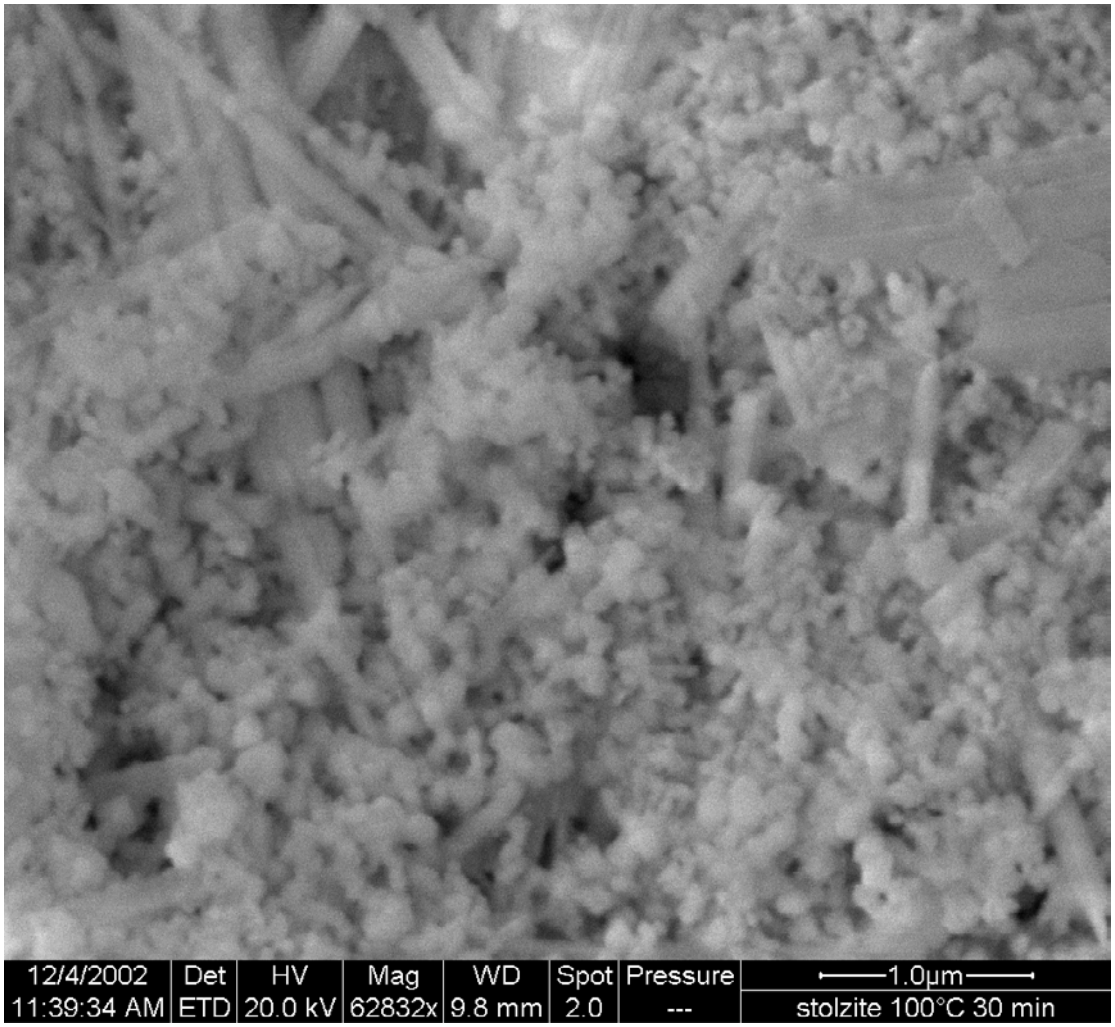

Fig. 3a SEM images of lead tungstate nanoparticles synthesised at 100°C for different times: (a) 30 minutes, (b) 1 hour, (c) 2 hours, (d-e) 150°C and 2hours

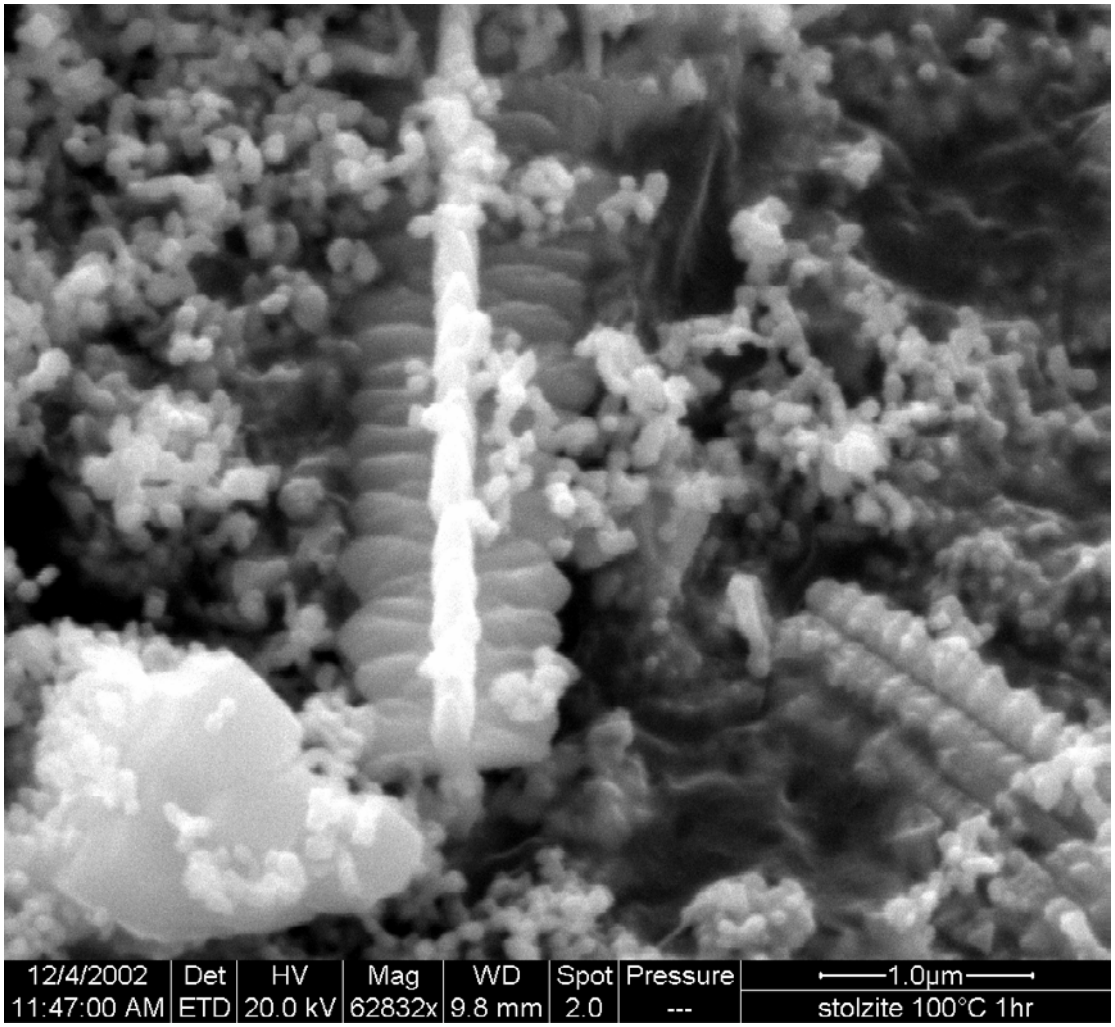
12/4/2002
11:47:00 AM
Det
ETD
HV
20.0 kV
Mag
62832x
WD
9.8 mm
Spot
2.0
Pressure

1.0µm
stolzite 100°C 1hr

Fig. 3b

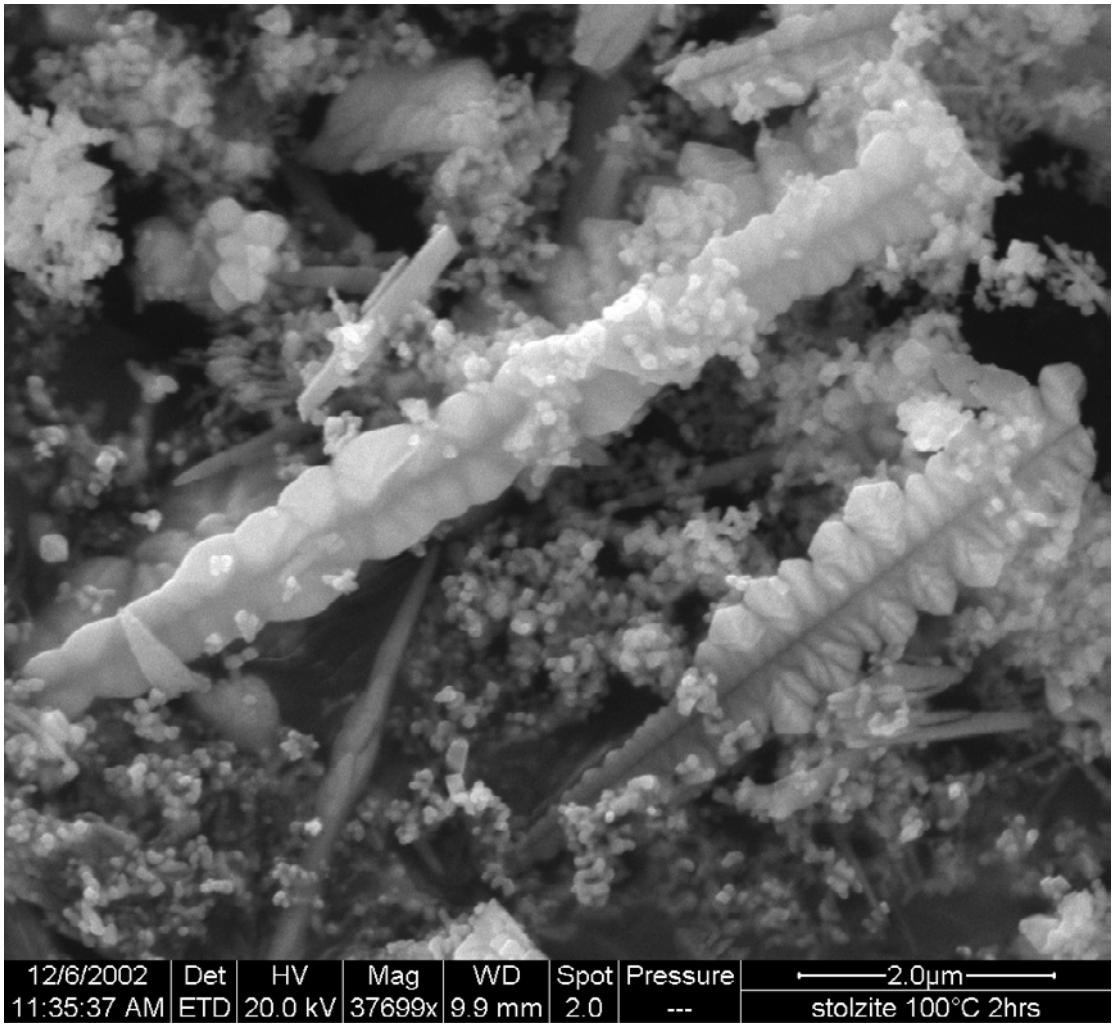
12/6/2002
11:35:37 AM
Det
ETD
HV
20.0 kV
Mag
37699x
WD
9.9 mm
Spot
2.0
Pressure

2.0µm
stolzite 100°C 2hrs

Fig. 3c

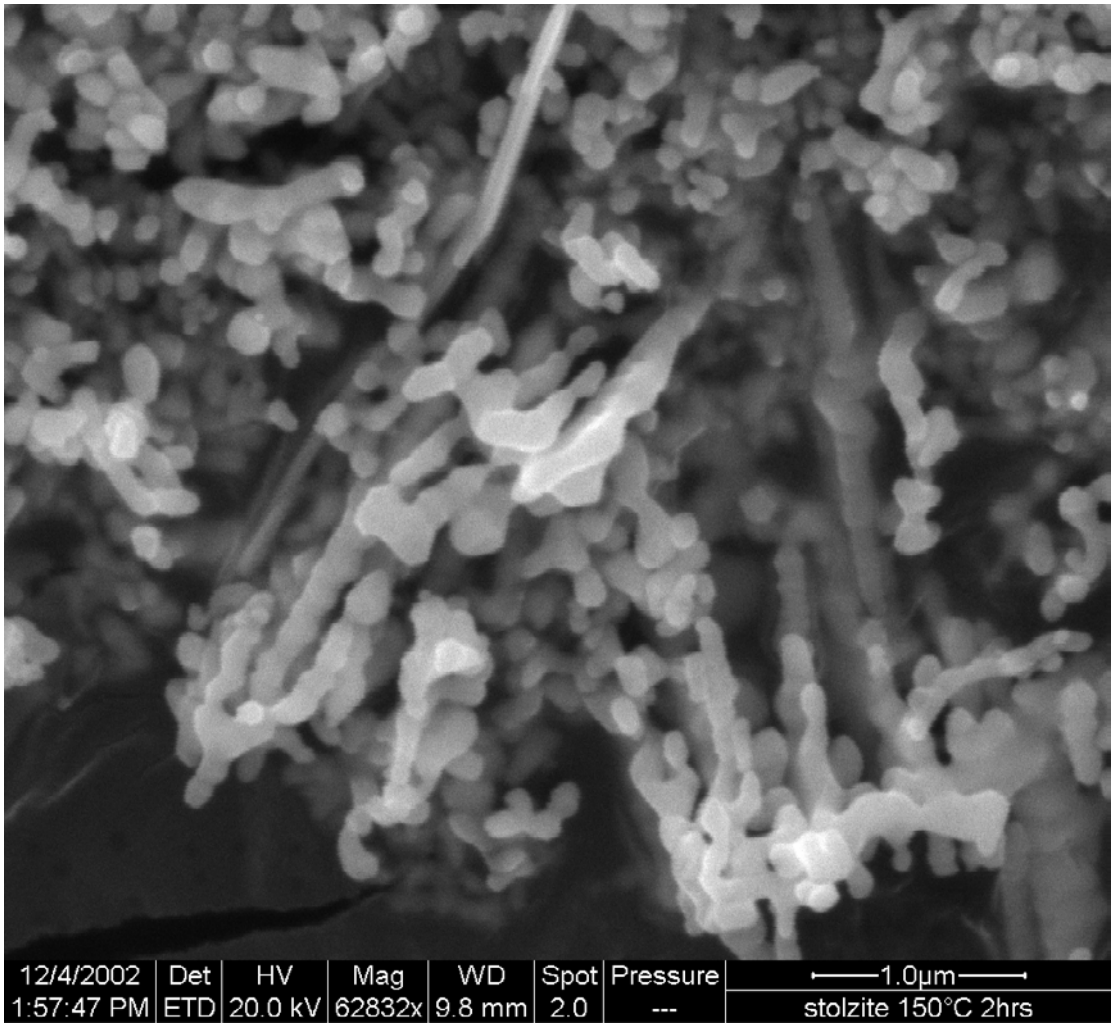
12/4/2002
1:57:47 PM
Det
ETD
HV
20.0 kV
Mag
62832x
WD
9.8 mm
Spot
2.0
Pressure

1.0µm
stolzite 150°C 2hrs

Fig. 3d

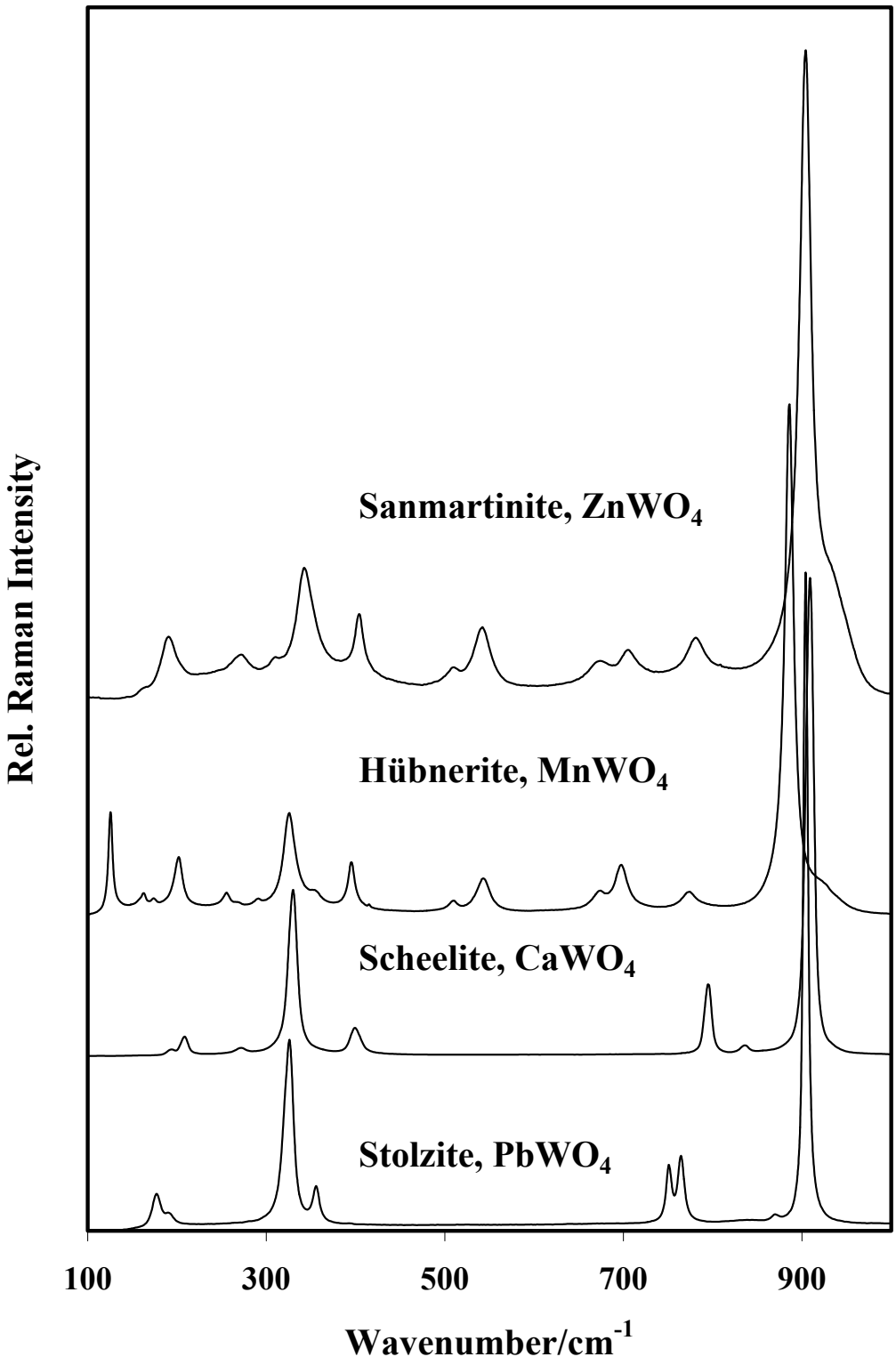

Fig. 4 Raman spectra between 100 and 1000 cm^{-1} of the synthetic tungstates